



**HAL**  
open science

# Experimental and Modeling of Tetracycline degradation in water in a Flow-Through Enzymatic monolithic reactor

Sher Ahmad, Wassim Sebai, Marie-Pierre Belleville, Nicolas Brun, Anne Galarneau, José Sanchez-Marcano

## ► To cite this version:

Sher Ahmad, Wassim Sebai, Marie-Pierre Belleville, Nicolas Brun, Anne Galarneau, et al.. Experimental and Modeling of Tetracycline degradation in water in a Flow-Through Enzymatic monolithic reactor. Environmental Science and Pollution Research, inPress, 29, 10.1007/s11356-022-21204-y . hal-03705382

**HAL Id: hal-03705382**

<https://hal.umontpellier.fr/hal-03705382v1>

Submitted on 27 Jun 2022

**HAL** is a multi-disciplinary open access archive for the deposit and dissemination of scientific research documents, whether they are published or not. The documents may come from teaching and research institutions in France or abroad, or from public or private research centers.

L'archive ouverte pluridisciplinaire **HAL**, est destinée au dépôt et à la diffusion de documents scientifiques de niveau recherche, publiés ou non, émanant des établissements d'enseignement et de recherche français ou étrangers, des laboratoires publics ou privés.

# **Experimental and Modeling of Tetracycline degradation in water in a Flow-Through Enzymatic monolithic reactor**

**Sher Ahmad<sup>1</sup>, Wassim Sebai<sup>1,2</sup>, Marie-Pierre Belleville<sup>1</sup>, Nicolas Brun<sup>2</sup>, Anne Galarneau<sup>2</sup>, José Sanchez-Marcano<sup>1\*</sup>**

<sup>1</sup>Institut Européen des Membranes, Univ Montpellier, CNRS, ENSCM, Montpellier, France.

<sup>2</sup>Institut Charles Gerhardt Montpellier, Univ Montpellier, CNRS, ENSCM, Montpellier, France.

\*Corresponding author:

*Tel: +33 467149149; Fax: +33 467149119; Email address: [Jose.Sanchez-Marcano@umontpellier.fr](mailto:Jose.Sanchez-Marcano@umontpellier.fr)*

1 **Abstract**

2 In this work, the laccase from *Trametes versicolor* was immobilized in highly porous silica monoliths (0.6  
3 cm diameter, 0.5 cm length). These monoliths feature a unique homogeneous network of interconnected  
4 macropores (20  $\mu\text{m}$ ) with mesopores (20 nm) in the skeleton and a high specific surface area (330  $\text{m}^2/\text{g}$ ). The  
5 enzymatic monoliths were applied to degrade tetracycline (TC) in model aqueous solutions (20 ppm). For  
6 this purpose, a tubular Flow-Through-Reactor (FTR) configuration with recycling was built. The TC  
7 degradation was improved with oxygen saturation, presence of degradation products and recirculation rate.  
8 The TC depletion reaches 50% in the FTR and 90% in a stirred tank reactor (CSTR) using crushed monoliths.  
9 These results indicate the importance of maintaining a high co-substrate concentration near active sites. A  
10 model coupling mass transfers with a Michaelis-Menten kinetics was applied to simulate the TC degradation  
11 in real wastewaters at actual TC concentration ( $2.8 \cdot 10^{-4}$  ppm). Simulation results show that industrial scale  
12 FTR reactor should be suitable to degrade 90% of TC in 5 h at a flow rate of 1 mL/min in a single passage  
13 flow configuration. Nevertheless, the process could certainly be further optimized in terms of laccase activity,  
14 oxygen supply near active sites and contact time.

15

16

17 **Key words.** Water treatment, Enzymatic silica monoliths, pharmaceuticals degradation, tetracycline  
18 degradation, Flow-Through-Reactor, Modelling, Scale-up.

19

20

## 21 1 Introduction

22 Pharmaceutical products (PPs) are found more and more frequently in the environment due to an increase in  
23 their consumption, because humans have a better access to medicines in conjunction with the aging of the  
24 population. Indeed, they can be found at very low concentrations ( $\mu\text{g L}^{-1}$ -  $\text{mg L}^{-1}$ ) in wastewaters (Halling-  
25 Sørensen et al., 1998), rivers (Burns et al., 2018), sediments (Kerrigan et al., 2018) and sea (Björlenius et al.,  
26 2018). Moreover, traditional wastewater treatment plants (WWTP) are inefficient to completely remove PPs,  
27 (Alvarino et al., 2018; Thiebault et al., 2017; Verlicchi et al., 2012). Therefore, PPs remain in WWTP  
28 effluents and as a consequence they can be transferred to underground or surface waters, which are among  
29 the main sources of drinking water (Bruce et al., 2010; de Jongh et al., 2012). Several tertiary treatments have  
30 been proposed to improve the removal of PPs from wastewaters, they include advanced oxidation treatments  
31 ( Kanakaraju et al., 2018; Kıldak and Doğan, 2018), physical adsorption (Rajapaksha et al., 2019 ; Rocha et  
32 al., 2020) or even enzymatic degradation.

33 Enzymatic degradation of PPs can be an alternative option among the other tertiary treatments named  
34 previously, since enzymes mediate biochemical reactions at a rapid rate under mild operating conditions (pH,  
35 temperature, solvents, and ionic strength). In particular, oxidoreductase enzymes such as laccases, tyrosinases  
36 and peroxidases have the ability to oxidize large variety of PPs like phenols, drugs, and hormones (Singh  
37 Arora and Kumar Sharma, 2010; Demarche et al., 2012; De Cazes et al., 2014). Nevertheless, enzymatic  
38 process can be expensive and unsustainable if enzymes are not recycled within the system.

39 Immobilization generally increases the stability of enzymes under reaction conditions while allowing their  
40 reuse and then reducing costs. (Zhang et al., 2015 Ji et al., 2017). Several immobilization techniques like  
41 adsorption, entrapment and encapsulation have been applied for enzyme immobilization on solid supports  
42 however it is observed that covalent immobilization enhances enzymes stability and long-term process  
43 sustainability (Zdarta et al., 2018). Along with nature of enzymes and immobilization techniques, choosing  
44 suitable solid support is also very essential in enzymatic process. Inorganic support materials like silica,  
45 zirconia, active carbons have high mechanical strength and temperature stability therefore are explored for  
46 immobilization of enzymes (Sadeghzadeh et al., 2020; Bebić et al., 2020; Zdarta et al., 2020).

47

48 The application of enzymatic reactors for PPs degradation has been explored with different configurations  
49 like packed bed reactors (Nguyen et al., 2016; Bilal and Iqbal, 2019), fluidized bed reactors (Lloret et al.,  
50 2012; Piao et al., 2019) as well as enzymatic membrane reactors (EMR) (de Cazes et al., 2014; Barrios-  
51 Estrada et al., 2018). EMRs have been widely studied for PPs degradation because they combine two  
52 functions in a single unit: filtration and enzymatic reaction (Sanchez Marcano and Tostsis, 2002; Sanchez  
53 Marcano, 2019). Nevertheless, EMRs can also present some drawbacks like membrane clogging or low  
54 reactivity because the amount of biocatalyst grafted on the separative layer of membranes is relatively low.

55 Ji et al., (2016) observed less than 10 % of carbamazepine degradation with laccase from *Trametes versicolor*  
56 in an EMR without using mediators. De Cazes et al., (2014) found only 56 % of tetracycline (TC) degradation  
57 in 24 h with laccase from *Trametes versicolor* immobilized on ceramic membranes. Similarly, Barrios-  
58 Estrada et al., (2018) found that only 33% of bisphenol-A was degraded in 24 h with an immobilized laccase  
59 on the same type of membranes. To overcome some of these disadvantages, meso-/macroporous monoliths  
60 have been recently applied for enzyme immobilization, the objective is to provide a big surface area to  
61 immobilize a large amount of enzymes, together with a macroporosity which allows low pressure drop while  
62 avoiding clogging (Ahmad et al., 2021; Biggelaar et al., 2019; Sebai et al., 2022). Moreover, as far as  
63 substrates are forced to flow through the monolith porosity the probability of contact with the biocatalyst is  
64 enhanced while allowing a precise control of the contact time (Sanchez Marcano, 2019). This configuration  
65 is called Flow-Trough-Reactor (FTR). Silica monoliths prepared by emulsion templating and presenting a  
66 large distribution of macropores (50 nm to 6  $\mu\text{m}$ ) have been recently used as supports in biocatalysis  
67 (Biggelaar et al., 2017, 2019). Another type of silica monoliths have been prepared by spinodal  
68 decomposition. They featured a narrow distribution of macropores and presented the advantage of an  
69 independent control of macropores (in the range 1 to 50  $\mu\text{m}$ ) and mesopores diameters (in the range 4 to 30  
70 nm, with a corresponding to surface area of 800 to 200  $\text{m}^2 \text{g}^{-1}$ , respectively) (Fajula and Galarneau, 2019;  
71 Galarneau et al., 2016b, 2016a).

72 There are few reported models of mass transport through monoliths. They consider the macroscopic structure  
73 and developed approaches for simulation of velocity fields, diffusion, and dispersion of chemical species  
74 within the porous structure (Jungreuthmayer et al., 2015; Meyers and Liapis, 1999; Tallarek et al., 2002).  
75 These models, which are based on morphology and real structure of porous monoliths, require high  
76 computational techniques like image processing techniques as well as relatively large computing times and  
77 costs (Jungreuthmayer et al., 2015). This assertion is especially true for large-scale geometries required for  
78 practical engineering problems. Furthermore, apart from the recent work of Ahmad et al., (2021), no work  
79 has been reported in the literature coupling a reaction kinetics with transport of species within macroporous  
80 silica monoliths for scale-up purposes.

81 The objective of this research work was to develop an original FTR configuration using enzymatic monoliths  
82 for PPs degradation and studying by modeling and simulation the possibility of scale-up of the FTR for this  
83 application. For this purpose the degradation of tetracycline (TC) was chosen as model molecule of PPs.  
84 Firstly, a lab scale set up was used for studying experimentally the enzymatic degradation of TC by laccase  
85 from *Trametes versicolor* covalently immobilized on silica monoliths with large homogeneous macropores  
86 ( $\sim 20 \mu\text{m}$ ) to assess low pressure drop and mesopores of 20 nm providing a large surface area ( $330 \text{m}^2 \text{g}^{-1}$ ) to  
87 improve enzymes immobilization. TC degradation tests were carried out in a tubular FTR configuration with  
88 recycling for the degradation of TC in aqueous solutions. Oxygen effect on TC degradation as well as the  
89 effect of TC degradation products on degradation rate were also studied. Moreover, a previous reported

90 model (Ahmad et al., 2021) coupling mass transfers with an apparent Michaelis-Menten kinetics, determined  
91 under oxygen saturation conditions, was applied to simulate the TC degradation in real wastewaters having  
92 a TC concentration six orders of magnitude lower than oxygen concentration at saturation conditions at 25  
93 °C. The developed model was employed to simulate the geometrical scale up of monoliths for the complete  
94 TC degradation at usual real wastewater concentrations at different flows. To our knowledge, it is the first  
95 time that such a study of TC degradation in a FTR has been carried out considering the influence of oxygen  
96 as co-substrate and the degradation products and performing the scale-up for an actual concentration of this  
97 antibiotic in wastewaters.

98

## 99 2 Materials and Methods

100 Silica monoliths with hierarchical porosity were synthesized and functionalized by amino groups for being  
101 used as solid support for covalent immobilization of laccases. The laccase-monoliths were then used for the  
102 removal of tetracycline (20 ppm) contained in water in batch and in flow through configuration. conditions  
103 using a recycling configuration. The effects of recirculation flow rate, of oxygen and presence of by-products  
104 were analyzed. Simulation was performed to evaluate the performance of laccase-monoliths for the removal  
105 of tetracycline in concentration ( $2.8 \cdot 10^{-4}$  ppm) found in real wastewaters and to determine the size of  
106 monoliths necessary to treat efficiently such effluents in flow condition using a single passage configuration.

### 107 2.1 Materials

108 Powdered commercial laccase (activity  $\geq 0.5 \text{ U mg}^{-1}$  according to the provider), Tetracycline (TC) ( $\geq 98.0\%$ ),  
109 Glutaraldehyde (GLU) (25% v/v) and 2,2'-azino-bis (3-ethylbenzothiazoline-6-sulphonic acid) (ABTS) were  
110 all purchased from Sigma-Aldrich, Germany.

111 Silica monoliths with macropores of 20  $\mu\text{m}$  and mesopores of 20 nm diameters (specific surface area of 330  
112  $\text{m}^2 \text{ g}^{-1}$ ) were prepared by a controlled sol-gel process with tetraethylorthosilicate (TEOS) and polyethylene  
113 glycol (PEO) 100 kDa in acidic solution ( $\text{HNO}_3$ ) followed by a basic treatment ( $\text{NH}_4\text{OH}$  0.1 M) at 100 °C  
114 for 24 h and then calcined at 550 °C for 8 h, according to a method previously reported (Galarneau et al.,  
115 2016a). The monoliths were then activated at 250 °C under vacuum for 4 h to remove water prior to be  
116 grafted with 3-aminopropylamine triethoxysilane (APTES) in ethanol under reflux (80 °C) overnight with an  
117 excess of 10 amino groups per  $\text{nm}^2$ . The resulting  $\text{NH}_2$ -monoliths presented a grafting density of  $1.5 \text{ NH}_2/\text{nm}^2$   
118 corresponding to an amount of 0.8 mmol  $\text{NH}_2/\text{g}$  and leading to a specific surface area of  $197 \text{ m}^2 \text{ g}^{-1}$ . The  
119  $\text{NH}_2$ -monoliths were then clad with a Teflon heat shrinkable gain at 180 °C for 2 h connected to stainless-  
120 steel tubing (Ahmad et al., 2021).

121 **2.2 Activation of monoliths and laboratory scale setup for TC degradation in water** Cladded NH<sub>2</sub>-  
 122 silica monoliths were activated with a GLU solution (4% v/v) prepared in citrate phosphate buffer (pH 7, 0.1  
 123 M). Then, monoliths were filled with 0.5 mL of laccase solution (5±1 U mL<sup>-1</sup>) prepared by solubilizing the  
 124 necessary amount of commercial powder of enzyme in the same citrate phosphate buffer. After  
 125 immobilization, the resulting laccase-monoliths were stored in the buffer solution (pH 7) at 4 °C. The  
 126 measurement of the enzymatic activity of laccase immobilized in monoliths, was carried out through the  
 127 oxidation of 1 mM solution of 2,2-azino-bis(3-ethylbenzothiazoline-6 sulfonic acid (ABTS) at pH = 4. For  
 128 this purpose, the laccase-monoliths were crushed, and experiments were carried out in a stirred tank reactor  
 129 (25-50 mL) under vigorous magnetic agitation at 200 rpm. The same methodology was applied for the  
 130 determination of kinetic constants of TC degradation. Immobilization methods and activity determination of  
 131 crushed laccase-monoliths were described in detail in a previous publication (Ahmad et al., 2021).

132 A laboratory scale set up for TC degradation (Figure 1) was built by connecting in series three cladded  
 133 enzymatic monoliths (0.6 cm diameter, 0.5 cm length, ~50 mg, each). A HPLC pump (Gibson model: 321,  
 134 France) allowed recycling a TC solution in between the monoliths and a reservoir. A pressure transducer  
 135 (Keller, 0-2 bar) was connected before the inlet of the monoliths to monitor the pressure changes during the  
 136 process. The temperature of the feed tank was controlled placing the feed tank in a thermostatically controlled  
 137 water bath. All the TC degradation tests were carried out in closed loop (complete recycling of the TC  
 138 solution (20 ppm)) because of low TC degradation in a single pass. A TC solution (20 ppm, 30 mL) was  
 139 flowed through the monoliths at three different flow rates (0.5, 1 and 5 mL min<sup>-1</sup>). In additional experiments,  
 140 air was bubbled in the feed tank solution at the air flow rate of 30-40 mL min<sup>-1</sup> to keep feed TC solution at  
 141 oxygen saturation (measured with a DO meter VisiFerm RS-485 from Himlton (Switzerland)). Based on the  
 142 macropore volumes of the monolith (3.41 mL/g), we can estimate the number of times (cycles) the solution  
 143 passes through the FTR built with three enzymatic monoliths in series (~150 mg) (Table 1):

144

145 **Table 1.** Number of cycles through the laccase-monoliths reactor as a function of flow rate

Flow rate (mL/min)	Number of cycles in 24h (V <sub>macro</sub> : 3.41 mL/g)
0.5	1409
1	2818
5	14090

146

147 The Reynolds number (Re) (Bird, et al, 1960) was calculated from the well known following equation:

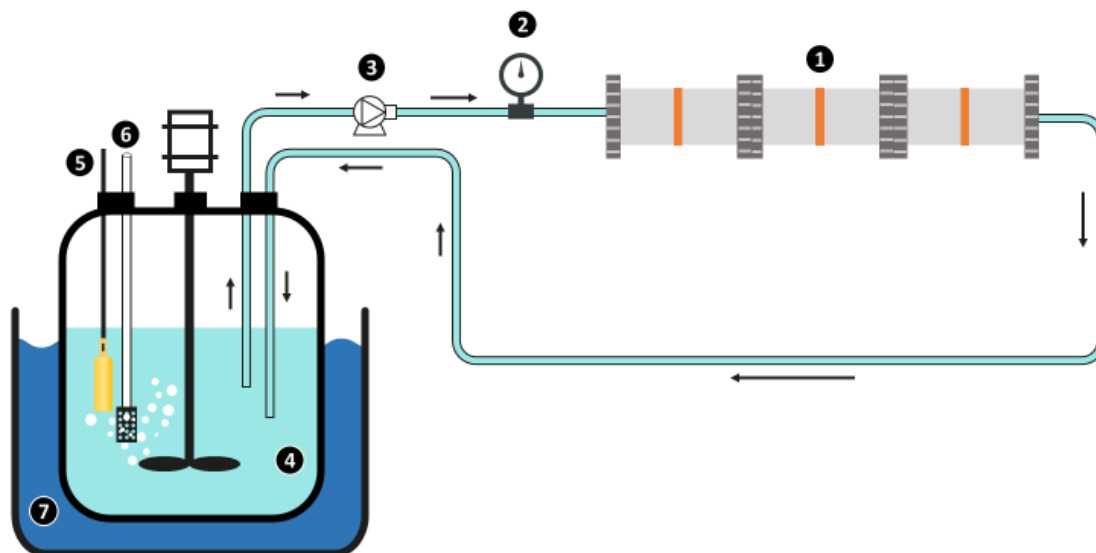


148  $Re = \frac{\rho u d_{macro}}{\mu}$  (1)

149 with  $\rho$  (0.997047 kg m<sup>-3</sup>) the density of water at 25 °C,  $\mu$  (0.000891 kg m<sup>-1</sup> s<sup>-1</sup>) the dynamic viscosity of water  
150 at 25 °C,  $d_{macro}$  (2 10<sup>-5</sup> m) the macropores mean diameter and  $u$  (m s<sup>-1</sup>) the velocity of water within  
151 macropores,  $u = V/A$  with  $V$  the flow rate (5 10<sup>-4</sup> to 5 10<sup>-3</sup> L min<sup>-1</sup>) and  $A$  the section of the monolith (6 mm  
152 diameter).

153 For comparison batch experiments were carried out with crushed laccase-monomoliths (~150 mg) in a stirred  
154 tank reactor (CSTR 50 mL) containing 30 mL of TC solution (20 ppm) under magnetic stirring (200 rpm).  
155 In this case also additional experiments were carried out by bubbling air in the solution at the air flow rate of  
156 30-40 mL min<sup>-1</sup> to maintain oxygen saturation conditions. Samples of 100  $\mu$ L were taken from feed tank  
157 every 30 min to measure the TC concentration evolution during 24 h by HPLC-MS analysis (Waters 2695  
158 separation module with micromass detector of Wythenshawe, Manchester, UK). Degradation products of TC  
159 were separated and identified by means of liquid chromatography coupled to high resolution mass  
160 spectrometer QExactive (LC-HRMS) equipped with a HESI ionization source operating in negative or  
161 positive ionization mode, in separate injections. Data acquisition was performed in data dependent scan  
162 where the 10 most intense ions from full scan ( $m/z$  50-600) were further fragmented with an isolation of 1.0  
163 Da at a collision energy of 30 a.u. Data results were processed manually with Xcalibur 3.1 software (IDAEA-  
164 CSIC laboratory, Spain).

165 Control experiments to study the effect of TC self-degradation or adsorption on the evolution of TC  
166 concentration were carried out with whole or crushed inactivated enzymatic monoliths. For this purpose,  
167 enzymatic monoliths were deactivated by heating in oven at 100 °C for 2 h.



168

169 **Figure 1.** Schematic draw of the laboratory scale set up for TC degradation with recycling. 1: reactor  
170 composed of three monoliths in series, 2: pressure transducer, 3: HPLC pump, 4: Stirred tank with TC  
171 solution, 5: air bubbling system, 6: thermocouple, 7: Thermostatic water bath.

## 172 3 Results and discussions

### 173 3.1 Effect of recirculation rate on TC degradation

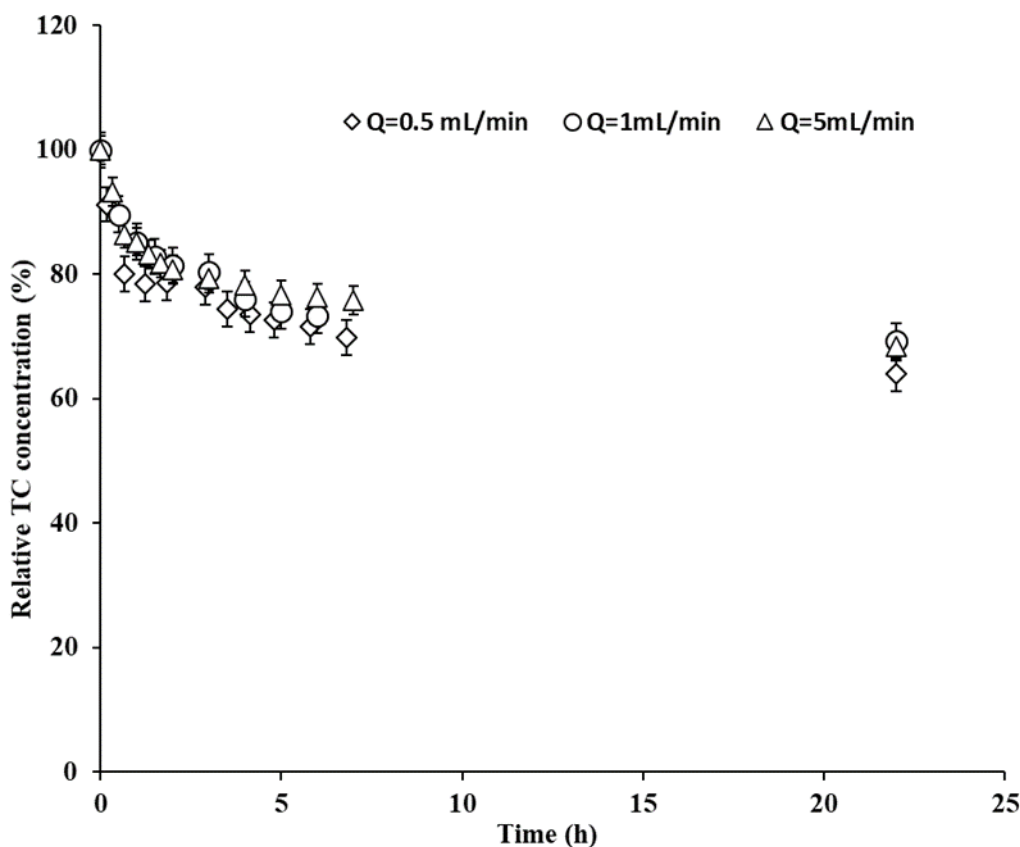
174 Recirculation rate in enzymatic reactor is an important parameter for continuous flow. When the recirculation  
175 rate is slow, the reaction can behave a similarly as non-continuous processes (Hamam and Budge, 2010) with  
176 a long contact time with the enzymes. When the recirculation rate is fast, more oxygen is is transported close  
177 to the enzymes, but the contact time is shorter. Therefore, it was important to determine the optimum flow  
178 rate for the TC degradation.

179 To study the effect of recirculation flow, TC degradation tests were carried out using the set up shown in  
180 Figure 1 at different recirculation flow rates from 0.5 to 5 mL min<sup>-1</sup> at 25 °C. For each test, fresh laccase-  
181 monoliths were used with initial TC solution concentration of 20 ppm and total volume of TC solution of 30  
182 mL. The decrease in relative TC concentration was similar for all flow-rates (Figure 2): 30% of the TC was  
183 degraded in the first five hours. For longer time reaction the degradation rate was extremely low (about 10%  
184 of additional degradation over the next 20 hours). This effect was observed with all tested recirculation flow

185 rates, which means that there was no effect of flow rate on the TC degradation. This indicates that the  
186 transport of substrates inside the reactors containing the enzymes immobilized on silica monoliths is  
187 governed by the self-diffusion in the mesopores and not by external mass transfer in the macropores.

188 The increase of the flow rate did not allow modifying the hydrodynamic flow regime. Indeed, the Reynolds  
189 number ( $Re$ ) calculated from Eq (1) for the recirculation flow rates of 0.5 to 5 mL min<sup>-1</sup> was ranged between  
190 0.01 - 0.1 and corresponded for all flow rates to a laminar flow regime (limit of the laminar flow regime ( $Re$   
191  $< 1$ ) (Bird et al, 1960). It can be concluded that the increase in flow rate was not high enough to further  
192 decrease possible external mass transfer resistances (decrease of boundary layers). In previous studies,  
193 Galarneau et al., (2016b) studied the dependence of flow rate on external mass transfer layer with silica  
194 monoliths for Diels-Alder reaction. They observed that productivity was increased by increasing the flow  
195 rate from 0.01 to 0.03 mL min<sup>-1</sup>. In another study, Jatoi et al., (2021) studied the effect of flow rate on  
196 external mass transfer limitations with silica monoliths loaded with Pt in the continuous-flow liquid-phase  
197 hydrogenation of *p*-Nitrophenol. They observed that for the range of flow rate from 1 to 8 mL min<sup>-1</sup> there  
198 was no effect on mass transfer limitations in macropores and attributed this behavior to the relative “high”  
199 flow rate applied. From these results it can be concluded that boundary layer reduction and optimum flow  
200 depends on several other factors like reaction rate, substrate concentration, pore size and porosity, which  
201 needs to be optimized as well.

202



203

204 **Figure 2.** TC degradation at different flow rates (0.5-5 mL min<sup>-1</sup>). Temperature: 25°C; TC initial  
 205 concentration of 20 ppm; total volume of TC solution of 30 mL, 15 U of enzymes in laccase-monomoliths.

206

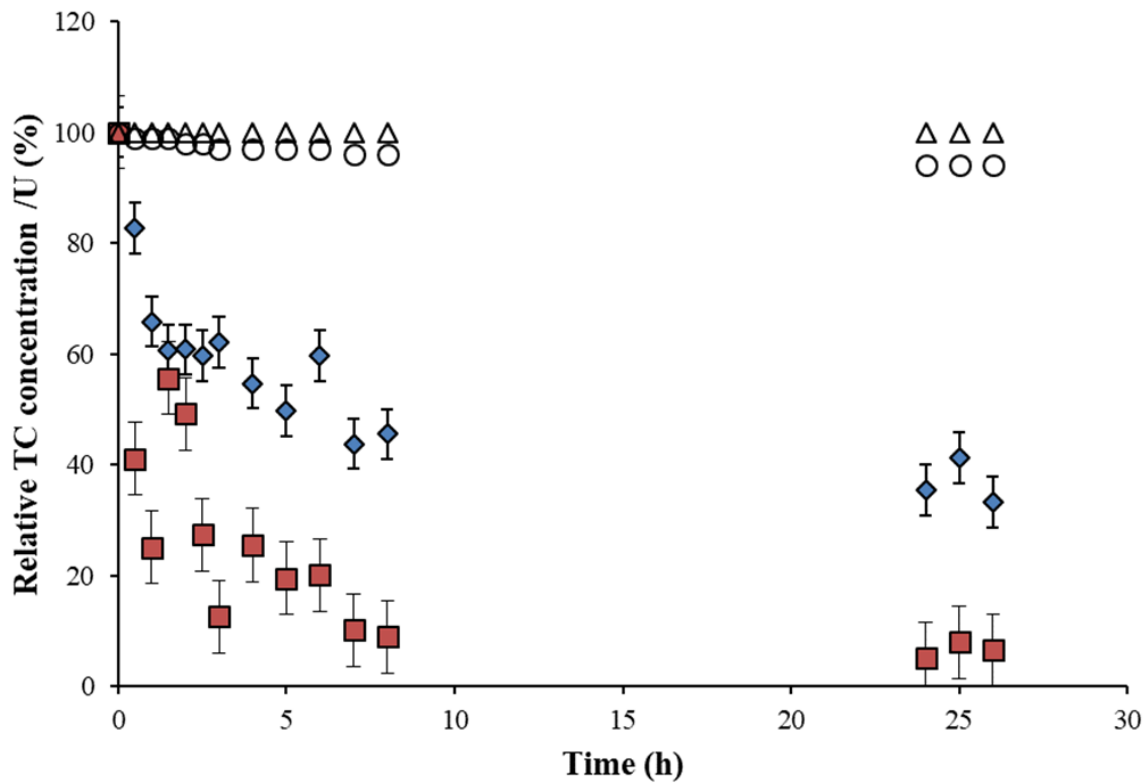
207 There are other possible explanations to the low experimental TC degradation (Figure 2). For example, the  
 208 process can be controlled by internal mass transfer, i. e. diffusion inside the mesopores, which can be  
 209 considered as stagnant regions in monoliths. In fact, silica monoliths feature skeletons with a thickness in the  
 210 range 5-15 μm, which contain an interconnected mesoporous structure where the major part of enzyme  
 211 molecules is immobilized. Therefore, the most part of reactive sites inside the mesoporous structure are only  
 212 accessible through the diffusion of substrates.

213

### 214 3.2 Effect of dissolved oxygen on TC degradation

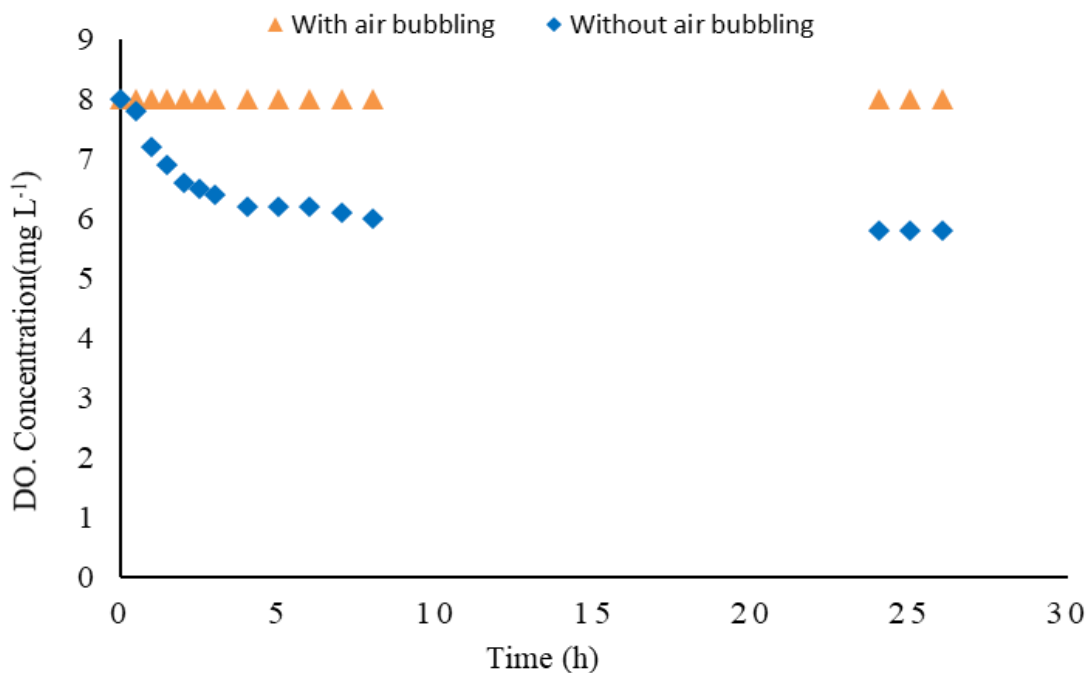
215 Laccases<sub>7</sub> are multicopper oxidases that catalyze the oxidation of different aromatic compounds with  
 216 molecular oxygen, which is concomitantly reduced to water (Nyanhongo et al., 2012). In order to study the  
 217 importance of the amount of oxygen available for the TC degradation, the effect of the addition of air bubbling  
 218 at a flow rate of 30-40 mL min<sup>-1</sup> was first studied in a stirred tank reactor with crushed monoliths as discussed

219 in section 2.2 (Figure 3). The concentration of the dissolved oxygen in the tank was measured during the  
220 experiments with and without air-bubbling (Figure 4).



221

222 **Figure 3.** Evolution of TC concentration with crushed laccase-monoliths in a stirred tank reactor, without  
223 (diamonds) and with (squares) air-bubbling. Control experiments with inactivated laccase-monoliths with  
224 (circles) and without (triangles) air bubbling. Initial TC concentration of 20 ppm in osmosed water (pH 6).  
225 Enzyme concentration of 18 U in the laccase-monoliths. Total volume 30 mL, temperature 25 °C.



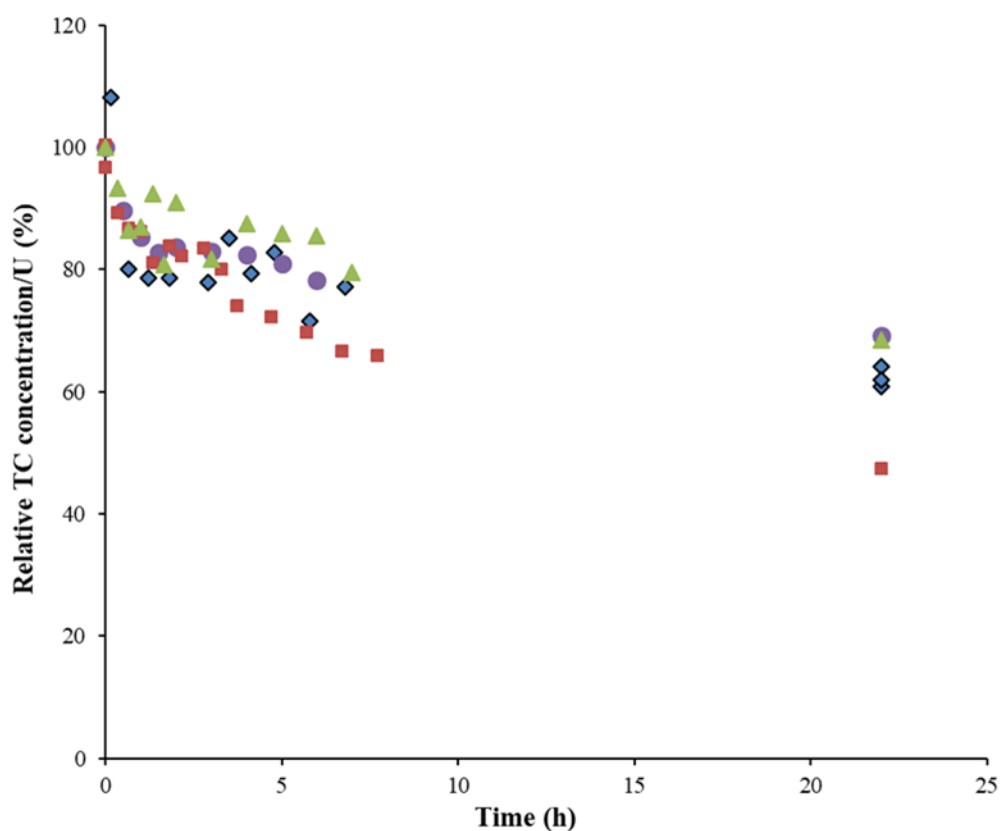
226

227 **Figure 4.** Evolution of dissolved oxygen (DO) concentration verse time in case of TC degradation test with  
 228 crushed laccase-monoliths in a stirred tank reactor with (triangles) or without (diamonds) air bubbling. Initial  
 229 TC concentration of 20 ppm in osmosed water (pH 6). Enzyme concentration of 18 U in the laccase-  
 230 monoliths. Total volume 30 mL, temperature 25 °C.

231

232 From Figure 3 it can be observed that for control tests (with inactivated laccase-monoliths) TC self-  
 233 degradation or adsorption (with or without air bubbling) was extremely low (less than 5%). Furthermore, For  
 234 the crushed active monoliths without air bubbling the TC degradation was 55% in the first 6 h, while with  
 235 air bubbling, the TC degradation reached more than 90% in the same period. These results show that oxygen  
 236 seems to be a limiting substrate for TC degradation. The same conclusion was found in literature (Ortner et  
 237 al., 2015) for the oxidation of lignins using laccase from *Trametes villosa*. The authors observed a rapid  
 238 decrease of oxygen concentration at the beginning of the reaction, which limited the oxidation of phenolic  
 239 compounds. They concluded that a sufficient oxygen concentration is necessary for an efficient laccase  
 240 oxidation process. In the present work, when the solution was bubbled with air, the dissolved oxygen (DO)  
 241 was always at saturation value ( $\sim 8.3 \text{ mg L}^{-1}$  at 25 °C) (Figure 4), which corresponded to an excess of 5.6  
 242 moles of oxygen/moles of TC. Without air bubbling, the DO concentration decreased of 20% in the first 6 h  
 243 concomitantly with the decrease of TC concentration (55%) to reach a steady-state of DO concentration of 6  
 244  $\text{mg L}^{-1}$ . The calculation of the number of moles of TC and oxygen ( $5.6 \cdot 10^{-6}$  and  $1.35 \cdot 10^{-6}$ , respectively)  
 245 indicates that a final molar ratio  $\text{O}_2/\text{TC}$  of 4, is therefore not enough to proceed to further oxidation. An  
 246 excess of at least 5.6  $\text{O}_2$  molecules per TC seems to be necessary for total TC oxidation.

247 The effect of air bubbling in the FTR was studied at two different flow rates (1 and 5 mL min<sup>-1</sup>) by bubbling  
248 air inside the feed tank (30-40 mL min<sup>-1</sup>) (Figure 5). Initial TC concentration for each experiment was 20  
249 ppm, the total volume of solution in the tank was 30 mL and the total activity of the 3 cladded laccase-  
250 monoliths was 12 U. For the flow rate of 5 mL min<sup>-1</sup>, the degradation of TC reached 50 % with air bubbling,  
251 while without air bubbling the TC degradation was only 30%. Similarly, for the flow rate of 1 mL min<sup>-1</sup>, the  
252 TC degradation was 40 and 30% with and without air bubbling, respectively. With air bubbling, TC  
253 degradation was slightly higher in the case of the larger flow rate (5 mL min<sup>-1</sup>) due to the larger amount of  
254 oxygen provided to the reactor. Nevertheless, this TC degradation ratio remains low compared to 90% TC  
255 degradation reached in a stirred tank reactor with air bubbling (Figure 5).



256

257 **Figure 5.** Evolution of TC concentration with laccase-monoliths under recycling flow at different flow rates  
258 without air bubbling (TC solution flow rates: circle, 1 mL min<sup>-1</sup>; triangle, 5 mL min<sup>-1</sup>) and with air bubbling  
259 (TC solution flow rates: diamonds, 1 mL min<sup>-1</sup>; squares, 5 mL min<sup>-1</sup>) at 25°C. Conditions: initial TC  
260 concentration of 20 ppm in osmosed water; total volume of TC solution of 30 mL; total activity of the laccase-  
261 monoliths of 12 U.

262

263 These results suggest the decrease of oxygen concentration near the bio-catalytic sites (which are located  
264 everywhere in the surface of monoliths, but mainly inside the mesoporosity), which limits the reaction rate

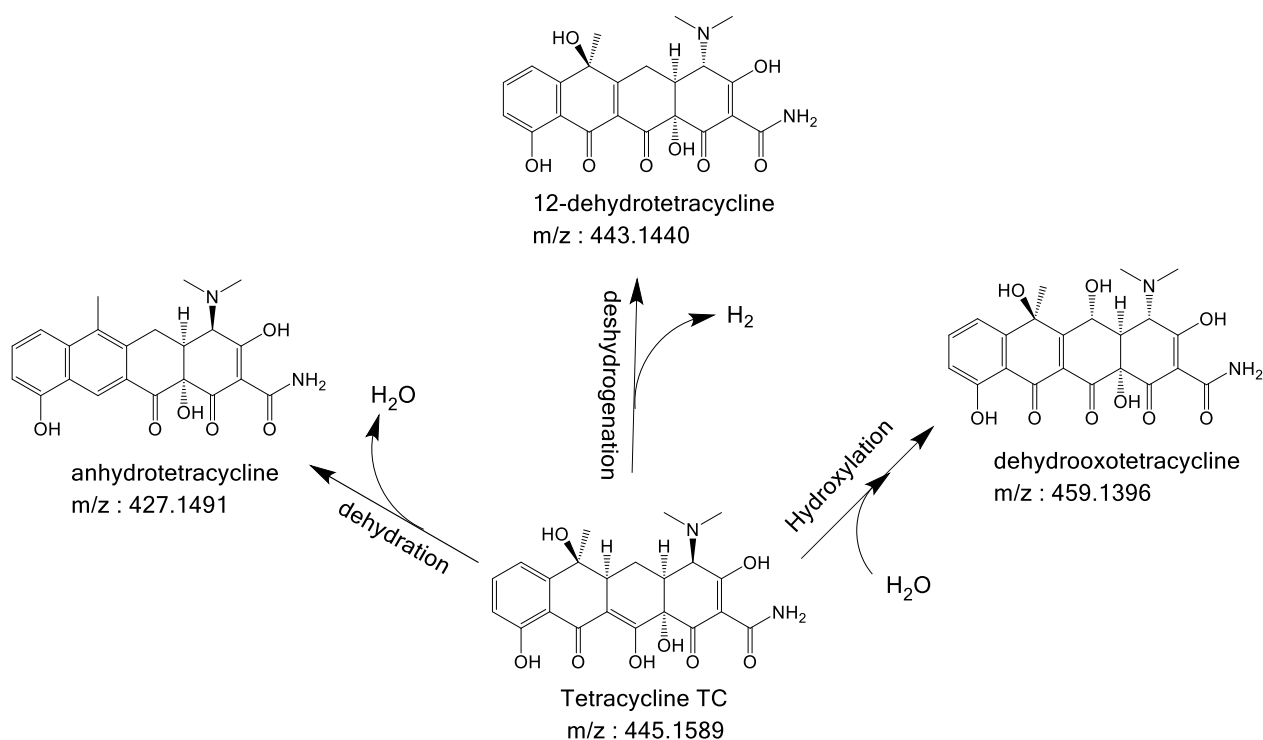
265 and the conversion in flow. Furthermore, maintaining a high oxygen concentration or even an excess of  
266 oxygen in the solution of the reservoir is not enough to enhance the conversion; this emphasizes that the  
267 decrease of co-substrate ( $O_2$ ) concentration near catalytic sites certainly controls the process.

268

### 269 3.3 Effects of TC degradation products

270 Many different TC degradation products were identified using the same laccase immobilized in ceramic  
271 membranes (De Cazes., et al., 2014). These products present a TC based structure like anhydrotetracycline,  
272 4-epi-anhydrotetracycline, dehydrooxotetracycline and 12-dehydrotetracycline (Llorca et al., 2015). In this  
273 study the main molecules identified by LC-HRMS (IDAEA-CSIC laboratory, Spain) during the degradation  
274 of TC are presented in Figure 6. One of the major products identified was dehydroxytetracycline ( $m/z =$   
275  $459.1396$ ) obtained after hydroxylation of the tetracycline. Some other products were identified coming from  
276 the loss of functional groups ( $-OH$ ,  $-NH_2$ , etc.) of the tetracycline molecule. However the gap in the mass  
277 balance between initial tetracycline and the amount of identified by-products indicates that the majority of  
278 tetracycline was polymerized (as is usually the case for phenolic compounds), or completely oxydized into  
279  $CO_2$  or transformed in other by-products, which were not detectable by LC-HRMS.

280



281

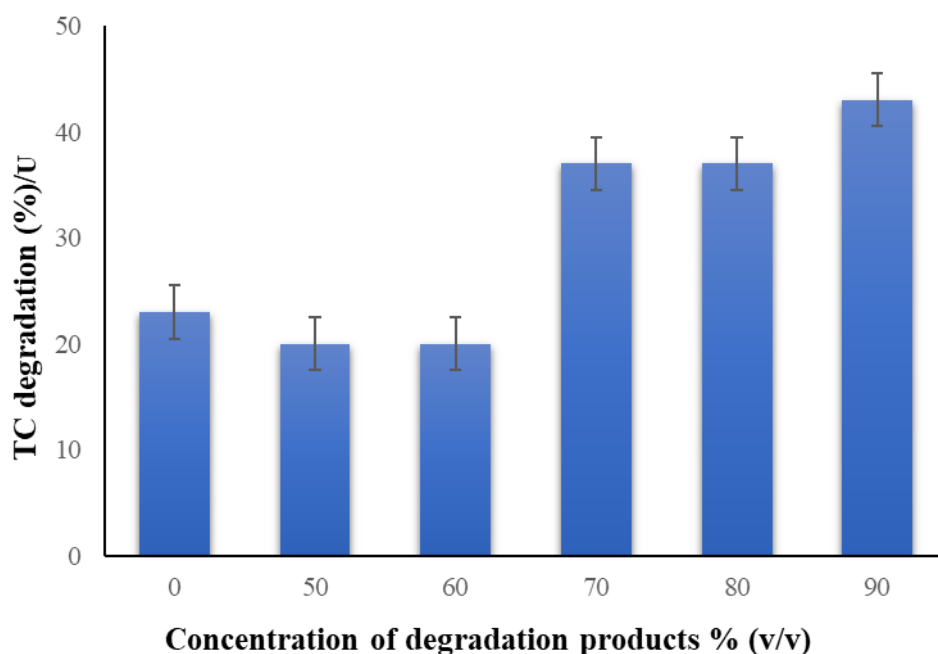
282 **Figure 6.** Degradation products of tetracycline and possible reaction pathways using laccase from *Trametes*  
283 *versicolor* immobilized on silica monolith.

284



285 As enzymes can be inhibited by the products of the enzymatic conversion (Jing et al., 2009; Barth et al.,  
286 2015), the effect of degradation products on TC degradation rate was studied with crushed monoliths and  
287 under vigorous stirring to avoid any influence of mass transport limitations. For this purpose, an initial TC  
288 degradation test was carried out for 24 h, with 50 mL of fresh TC solution (20 ppm) and a total enzymatic  
289 activity of crushed monoliths of 6 U. After 24 h of reaction (without air bubbling), the reaction mixture  
290 (unconverted TC + degradation products) was separated from the immobilized enzymes by filtration.  
291 Afterward, a series of TC degradation experiments were carried out at different concentrations of degradation  
292 products by adding a volumetric fraction (50-90%) of the reaction mixture obtained from the initial  
293 experiment to a fresh TC solution (up to reach an initial TC concentration of 20 ppm) mixed with a fresh  
294 crushed enzymatic monolith (6 U). The results obtained are shown in Figure 7. It is important to notice that  
295 a lower degree of TC degradation (20%) was observed in comparison to the results (60% degradation)  
296 reported in Figure 3. This is due to the use of a lower enzymatic monolith activity (6 U instead of 18 U).

297



298

299 **Figure 7.** Effect of the amount of TC degradation products on TC degradation in batch. Initial TC  
300 concentration of 20 ppm; crushed laccase-monolith (6 U); temperature 25 °C; reaction time of 24 h.

301

302 The main result of this series of experiments is the enhancement of TC degradation with the increase of  
303 concentration of degradation products. Without degradation products and until a concentration of 60% of  
304 degradation products, TC degradation is around 20% in 24 hours, whereas for more than 70% of degradation  
305 products present in the solution, TC degradation reaches 40% after 24 hours. These results show that the TC  
306 degradation products formed did not inhibit the TC degradation, but in opposite they enhanced the conversion

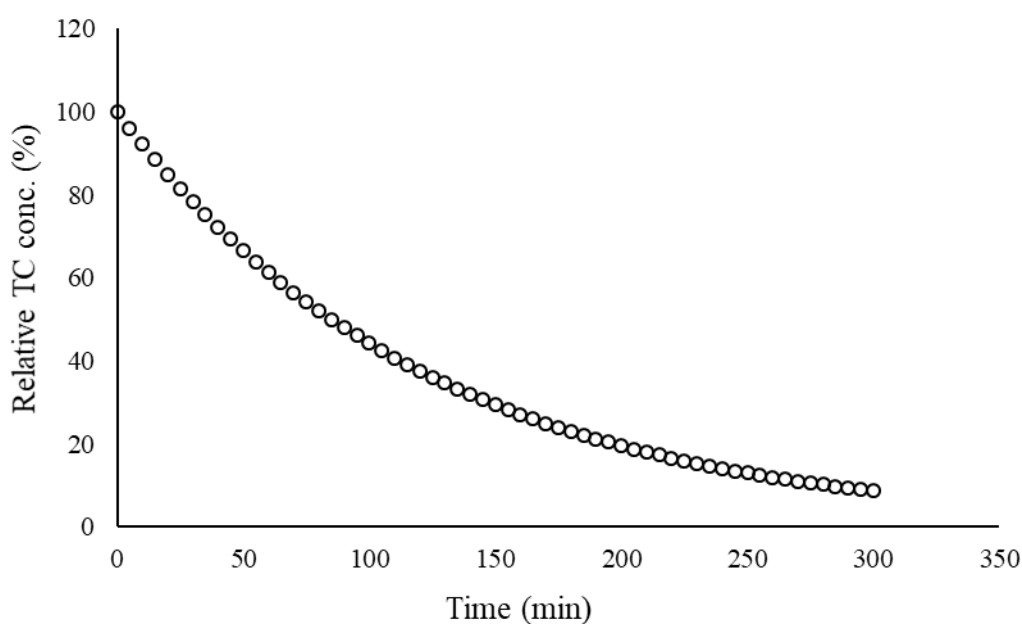
307 when their concentration reached a minimum level. A similar phenomenon has been recently observed by  
308 Parra Guardado et al., (2019) and has been explained by the fact that some products of the reaction can act  
309 as redox mediators enhancing the enzyme reactivity and the conversion. This could also explain the higher  
310 degradation rate of TC (by a factor 2) obtained in the stirred tank reactor in comparison to the FTR, where  
311 degradation products do not spend enough time in the enzyme vicinity.

312

### 313 **3.4 Application of a model for simulation of TC degradation in actual wastewater concentrations** 314 **and proposed scale up of monolith system**

315 In a previous work (Ahmad et al., 2021) reported a computational fluid dynamics (CFD) model allowing  
316 computing TC degradation. The model was built coupling an apparent Michaelis-Menten reaction kinetics  
317 of immobilized enzymes, flow hydrodynamics within the FTR and a dynamic mass balance on feed tank. As  
318 far as this model was built in conditions of oxygen saturation conditions and with a reaction kinetics, which  
319 only takes into account TC and not oxygen, it should not be applied for TC concentrations as high as used in  
320 this work (20 ppm). Indeed it was demonstrated here that oxygen becomes rapidly a limiting substrate.  
321 However, in some municipal wastewaters the TC concentration currently encountered is very low ( $2.8 \cdot 10^{-4}$   
322 ppm) (Abejón et al., 2015b; Danner et al., 2019). Thus, in this case and considering the saturation  
323 concentration of oxygen at 25 °C ( $8 \text{ mg L}^{-1}$ ), the concentration of  $\text{O}_2$  ( $\text{O}_2/\text{TC} = 4 \cdot 10^5$ ) would be five orders  
324 of magnitude larger than the requirement previously founded ( $\text{O}_2/\text{TC} = 5.6$ ). Under such conditions, we can  
325 consider that oxygen is no longer a limiting substrate and then the model can be reasonably applied for  
326 simulation purposes.

327



328

329 **Figure 8.** Simulated degradation of TC at actual initial TC concentration ( $2.8 \cdot 10^{-4}$  ppm) found in wastewater  
 330 in a FTR. Simulation conditions: flow rate ( $1 \text{ mL min}^{-1}$ ), continuous recycled mode, Temperature  $25 \text{ }^{\circ}\text{C}$ , 15  
 331 U of enzymatic activity in the monoliths.

332

333 The simulation of the TC degradation carried out with the FTR (3 monoliths in series of 0.6 cm diameter and  
 334 0.5 cm length, each) shows that for real TC concentration ( $2.8 \cdot 10^{-4}$  ppm) a removal of 90% of TC was reached  
 335 in 5 h at a flow rate of  $1 \text{ mL min}^{-1}$  with a recycling configuration (see Figure 8). Taking account of these  
 336 results, we then proposed to determine the minimum size of a monolith that allows a complete degradation  
 337 of the TC in only one passage (without recycling) through the FTR. For this purpose, monoliths with different  
 338 size (length and diameter ranged in between 5-50 cm and 1-20 cm, respectively) were considered for  
 339 simulations (Table 2). When the size of monoliths is increased the conversion is enhanced. For example, for  
 340 a single pass, when the monolith geometry was set at 5 cm length and 1 cm diameter only 0.5% of initial TC  
 341 was converted. However, with monoliths of 50 cm length and 20 cm diameter it was possible to completely  
 342 degrade TC at a flow rate of  $1 \text{ mL min}^{-1}$ . These theoretical “large-scale monoliths” were then used for further  
 343 simulations.

344

345 **Table 2.** Effect of the scale up of the silica monoliths (by increasing the length and diameter of the monoliths)  
 346 towards TC degradation.

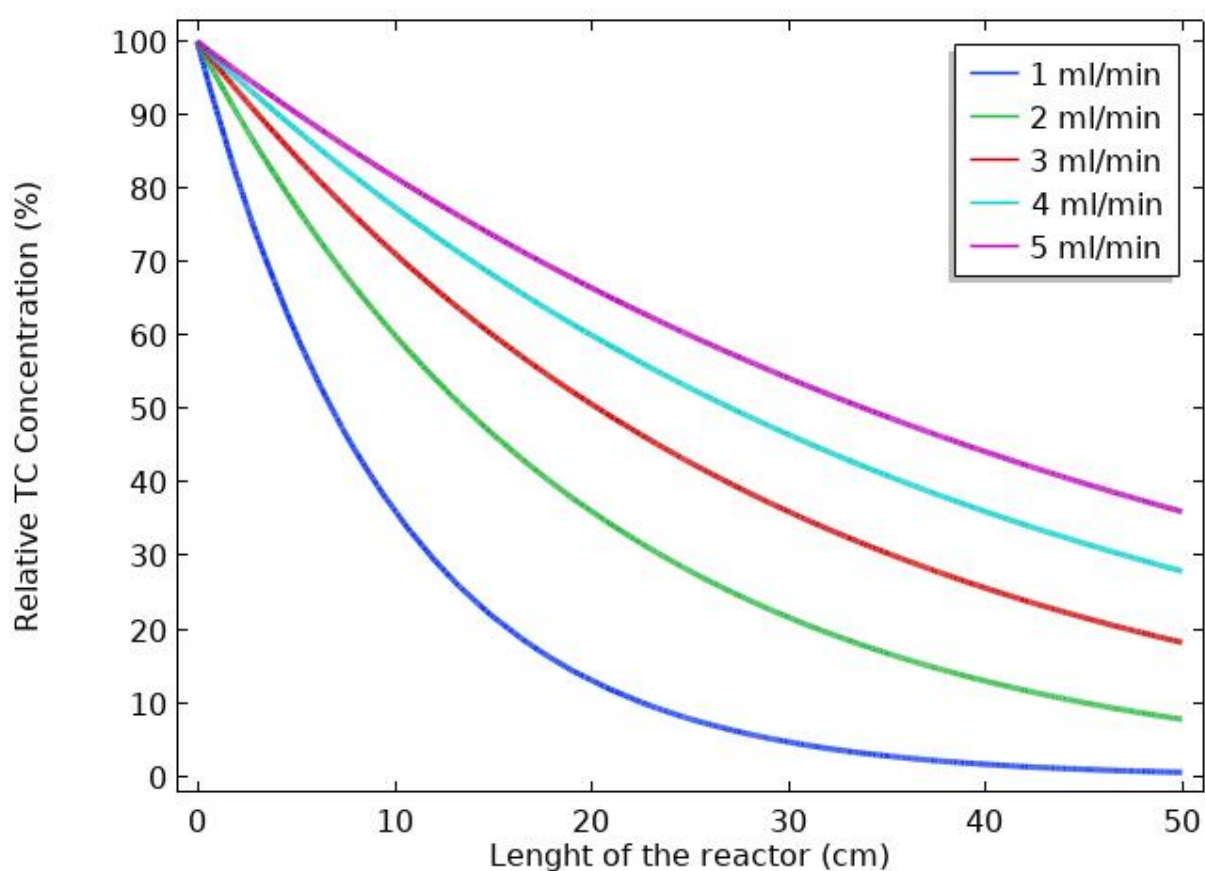
Length (cm)	Diameter (cm)	Inlet concentration (ppm) $\times 10^{-4}$	TC Outlet concentration (ppm) $\times 10^{-4}$	TC conversion in a single pass (%)
0.15	0.06	2.8	2.79	0.3
5	2	2.8	2.78	0.7
10	4	2.8	2.68	4
15	6	2.8	2.43	13
20	8	2.8	2.01	28
25	10	2.8	1.34	52
<b>50</b>	<b>20</b>	2.8	0	<b>100</b>

347

348 The TC conversion along the length of the optimum reactor (20 cm diameter, 50 cm length) was then studied  
 349 at different flow rates (Figure 9). Complete TC degradation was achieved at the flow rate of  $1 \text{ mL min}^{-1}$ .

350 However, it can be observed that the rate of TC depletion in the last 15 cm was relatively low; this last section  
351 of the monolith is not enough efficient. For flow rates higher than 1 mL min<sup>-1</sup>, TC conversion decreases up  
352 to 50% at a flow rate of 5 mL min<sup>-1</sup> (Figure 9). In fact, the global process is controlled by reaction kinetics  
353 and at high flow rates, the residence time is too low to reach a complete TC depletion. However, as real  
354 wastewater fluxes are extremely high (600-70,000 m<sup>3</sup>/day) a compromise must be found between the level  
355 of TC depletion, the contact time and process effectiveness. For this, an optimization has to be carried out  
356 with multi-objective programming like Pareto optimality, this analysis has to be coupled with the cost of the  
357 process (Abejón et al., 2015b).

358



359

360 **Figure 9.** Relative tetracycline concentration along the length of the reactor from inlet to outlet at different  
361 TC flow rates from 1 to 5 mL min<sup>-1</sup>. Reactor length: 50 cm, diameter: 20 cm; Inlet TC concentration: 2.8 10<sup>-4</sup>  
362 ppm; Reaction rate: 4.4 10<sup>-5</sup> μmol L<sup>-1</sup> min<sup>-1</sup>.

363

## 364 Conclusions

365 Biocatalytic reactors were built by grafting laccase into the mesopores of macroporous silica monoliths. The  
366 depletion of tetracycline (TC) (20 ppm) in aqueous solutions was carried out in a tubular flow through reactor

367 (FTR) configuration (3 monoliths in series of 0.6 cm diameter and 0.5 cm length, each) with recycling in a  
368 reservoir tank. Only 30-40% of TC was degraded during the first 5 h and then the conversion slowed down  
369 to a threshold. The increase of flow rate from 0.5 to 5 mL min<sup>-1</sup> did not change TC depletion showing that  
370 the phenomenon was not due to external mass transfer limitation, but rather to diffusion limitation of  
371 substrates inside the mesopores. Experiments performed in stirred tank reactors (CSTR) with crushed  
372 monoliths showed a higher TC depletion of 55% in 6 h, which was increased to 90% when the solution was  
373 bubbled with air. This showed that O<sub>2</sub> is a limiting substrate for this reaction and that a molar excess of at  
374 least 5.6 O<sub>2</sub>/TC is necessary for a complete TC depletion. In FTR configuration, the addition of air-bubbling  
375 in the reservoir lead to an increase of TC depletion of only 10%, with a maximum of 50% at flow rate of 5  
376 mL min<sup>-1</sup>, this result indicates that oxygen limitations are enhanced in FTR configuration due to the mass  
377 transport limitations inside the mesopores. It was observed that the presence of by-products of degradation  
378 increases the TC depletion, this result could be explained by a possible the role of redox mediators of such  
379 by-products. In real municipal wastewater TC concentration is very low (2.8 10<sup>-4</sup> ppm) and O<sub>2</sub> will be no  
380 more a limiting substrate as its excess of 5 orders of magnitude higher than TC. The modeling of FTR showed  
381 that in such conditions TC depletion should reach 90% in 5 h at a flow rate of 1 mL min<sup>-1</sup> in a recirculating  
382 flow mode. The model allowed to predict that a monolith of 20 cm diameter and 50 cm length could be used  
383 for a total depletion of TC in a single pass (without recirculation) at a flow rate of 1 mL/min. However for  
384 higher flow rates (as the one encountered in real wastewater treatments) the decrease of the TC depletion was  
385 noticed. This is due by the fact that the depletion is governed by the reaction kinetic of the laccase. Further  
386 improvement on laccase activity could contribute to optimize the process. New monolithic configurations  
387 and processes have to be designed in order to feed oxygen continuously inside the porosity.

388

#### 389 **Declarations**

390

#### 391 **Ethics approval and consent to participate**

392 Not applicable

393

#### 394 **Consent for publication**

395 Not applicable

396

397 **Availability of data and materials**

398 The datasets used and/or analyzed during the current study are available from the corresponding author on  
399 reasonable request, additional information and results are given in supplementary material.

400

401 **Competing interests**

402 The authors declare that they have no competing interests

403

404 **Funding**

405 This work was founded by The Agence Nationale de la Recherche (ANR, France) under the frame of the  
406 project MUSE ANR-16-IDEX-0006 project DEMEMO. The scholarship of Mr. S. Ahmad was provided  
407 by the Higher Education Commission, Pakistan

408

409 **Authors' contributions**

410 Sher Ahmad and Wassim Sebai carried out the experimental work, synthesis of monoliths and enzymatic  
411 degradation of tetracycline, Marie-Pierre Belleville designed degradation experiments and contributed to  
412 the scientific discussion, Nicolas Brun, designed monoliths synthesis and contributed to the scientific  
413 discussion, Anne Galarneau and Jose Sanchez Marcano supervised all of the work, contributed with the  
414 discussions and wrote the whole manuscript. All of the authors revised the manuscript.

415

416 **Acknowledgements.** The authors acknowledge the ANR French agency, which founded the project  
417 DEMEMO under the number MUSE ANR-16-IDEX-0006. Mr. S. Ahmad acknowledges the Higher  
418 Education Commission, Pakistan for the PhD scholarship. The authors wish to acknowledge the support  
419 from the chemistry platform of campus in Montpellier (Plateform MEA University of Montpellier), where  
420 SEM has been performed

421 **References**

422

423 Abejón, R., Belleville, M.P., Sanchez-Marcano, J., 2015a. Design, economic evaluation and optimization  
424 of enzymatic membrane reactors for antibiotics degradation in wastewaters. *Sep. Purif. Technol.* 156,  
425 183–199. <https://doi.org/10.1016/j.seppur.2015.09.072>

426 Abejón, R., De Cazes, M., Belleville, M.P., Sanchez-Marcano, J., 2015b. Large-scale enzymatic  
427 membrane reactors for tetracycline degradation in WWTP effluents. *Water Res.* 73, 118–131.  
428 <https://doi.org/10.1016/j.watres.2015.01.012>

429 Ahmad, S., Sebai, W., Belleville, M.-P., Brun, N., Galarneau, A., Sanchez-Marcano, J., 2021. Enzymatic  
430 monolithic reactors for micropollutants degradation. *Catal. Today*, 1st International Conference on  
431 Unconventional Catalysis, Reactors and Applications: Catalysis Beyond the Reactor 362, 62–71.  
432 <https://doi.org/10.1016/j.cattod.2020.04.048>

433 Almomani, F.A., Shawaqfah, M., Bhosale, R.R., Kumar, A., 2016. Removal of emerging pharmaceuticals  
434 from wastewater by ozone-based advanced oxidation processes. *Environ. Prog. Sustain. Energy* 35,  
435 982–995. <https://doi.org/10.1002/ep.12306>

436 Alvarino, T., Lema, J., Omil, F., Suárez, S., 2018. Trends in organic micropollutants removal in  
437 secondary treatment of sewage. *Rev. Environ. Sci. Biotechnol.* 17, 447–469.  
438 <https://doi.org/10.1007/s11157-018-9472-3>

439 Barrios-Estrada, C., Rostro-Alanis, M. de J., Parra, A.L., Belleville, M.-P., Sanchez-Marcano, J., Iqbal,  
440 H.M.N., Parra-Saldívar, R., 2018. Potentialities of active membranes with immobilized laccase for  
441 Bisphenol A degradation. *Int. J. Biol. Macromol.* 108, 837–844.  
442 <https://doi.org/10.1016/j.ijbiomac.2017.10.177>

443 Barth, M., Oeser, T., Wei, R., Then, J., Schmidt, J., Zimmermann, W., 2015. Effect of hydrolysis products  
444 on the enzymatic degradation of polyethylene terephthalate nanoparticles by a polyester hydrolase  
445 from *Thermobifida fusca*. *Biochem. Eng. J.* 93, 222–228. <https://doi.org/10.1016/j.bej.2014.10.012>

446 Bebić, J., Banjanac, K., Čorović, M., Milivojević, A., Simović, M., Marinković, A., Bezbradica, D., 2020.  
447 Immobilization of laccase from *Myceliophthora thermophila* on functionalized silica nanoparticles:  
448 Optimization and application in lindane degradation. *Chin. J. Chem. Eng.* 28, 1136–1144.  
449 <https://doi.org/10.1016/j.cjche.2019.12.025>

450 Biggelaar, L. van den, Soumillion, P., Debecker, D., 2019. Continuous Flow Mode Biocatalytic  
451 Transamination Using Macrocellular Silica Monoliths: Optimizing Support Functionalisation and  
452 Enzyme Grafting. <https://doi.org/10.26434/chemrxiv.7853552.v1>

453 Bilal, M., Iqbal, H.M.N., 2019. Lignin peroxidase immobilization on Ca-alginate beads and its dye  
454 degradation performance in a packed bed reactor system. *Biocatal. Agric. Biotechnol.* 20, 101205.  
455 <https://doi.org/10.1016/j.bcab.2019.101205>

456 Bird, R.B., Stewart, W.E., Lightfoot, E.N., 1960. *Transport phenomena*. New York: Wiley.

457 Björlenius, B., Ripszám, M., Haglund, P., Lindberg, R.H., Tysklind, M., Fick, J., 2018. Pharmaceutical  
458 residues are widespread in Baltic Sea coastal and offshore waters – Screening for pharmaceuticals and  
459 modelling of environmental concentrations of carbamazepine. *Sci. Total Environ.* 633, 1496–1509.  
460 <https://doi.org/10.1016/j.scitotenv.2018.03.276>

461 Burns, E.E., Carter, L.J., Kolpin, D.W., Thomas-Oates, J., Boxall, A.B.A., 2018. Temporal and spatial  
462 variation in pharmaceutical concentrations in an urban river system. *Water Res.* 137, 72–85.  
463 <https://doi.org/10.1016/j.watres.2018.02.066>

464 Cabana, H., Alexandre, C., Agathos, S.N., Jones, J.P., 2009. Immobilization of laccase from the white rot  
465 fungus *Corioliopsis polyzona* and use of the immobilized biocatalyst for the continuous elimination of  
466 endocrine disrupting chemicals. *Bioresour. Technol.* 100, 3447–3458. <https://doi.org/10.1007/s10103-009-0744-6>

468 Danner, M.-C., Robertson, A., Behrends, V., Reiss, J., 2019. Antibiotic pollution in surface fresh waters:  
469 Occurrence and effects. *Sci. Total Environ.* 664, 793–804.  
470 <https://doi.org/10.1016/j.scitotenv.2019.01.406>

471 de Cazes, M., Belleville, M.-P., Petit, E., Llorca, M., Rodríguez-Mozaz, S., de Gunzburg, J., Barceló, D.,  
472 Sanchez-Marcano, J., 2014. Design and optimization of an enzymatic membrane reactor for  
473 tetracycline degradation. *Catal. Today, Proceedings of the 11th International Conference on Catalysis  
474 in Membrane Reactors* 236, 146–152. <https://doi.org/10.1016/j.cattod.2014.02.051>

475 Demarche, P., Junghanns, C., Nair, R.R., Agathos, S.N., 2012. Harnessing the power of enzymes for  
476 environmental stewardship. *Biotechnol. Adv.* 30, 933–953.  
477 <https://doi.org/10.1016/j.biotechadv.2011.05.013>

478 François Fajula, Anne Galarneau, 2019. Combining Phase Separation with Pseudomorphic  
479 Transformation for the Control of the Pore Architecture of Functional Materials: A Review. *Pet. Chem.*  
480 59, 761–769. <https://doi.org/10.1134/S0965544119080061>

481 Galarneau, A., Abid, Z., Said, B., Didi, Y., Szymanska, K., Jarzębski, A., Tancret, F., Hamaizi, H.,  
482 Bengueddach, A., Di Renzo, F., Fajula, F., 2016a. Synthesis and Textural Characterization of  
483 Mesoporous and Meso-/Macroporous Silica Monoliths Obtained by Spinodal Decomposition.  
484 *Inorganics* 4, 9. <https://doi.org/10.3390/inorganics4020009>

485 Galarneau, A., Sachse, A., Said, B., Pelisson, C.-H., Boscaro, P., Brun, N., Courtheoux, L., Olivi-Tran, N.,  
486 Coasne, B., Fajula, F., 2016b. Hierarchical porous silica monoliths: A novel class of microreactors for  
487 process intensification in catalysis and adsorption. *Comptes Rendus Chim., Emerging Chemistry in  
488 France* 19, 231–247. <https://doi.org/10.1016/j.crci.2015.05.017>

489 Goi, A., 2005. Advanced oxidation processes for water purification and soil remediation, Thesis on  
490 chemistry and chemical engineering. TTU Press, Tallinn.

491 Halling-Sørensen, B., Nors Nielsen, S., Lanzky, P.F., Ingerslev, F., Holten Lützhøft, H.C., Jørgensen, S.E.,  
492 1998. Occurrence, fate and effects of pharmaceutical substances in the environment- A review.  
493 *Chemosphere* 36, 357–393. [https://doi.org/10.1016/S0045-6535\(97\)00354-8](https://doi.org/10.1016/S0045-6535(97)00354-8)

494 Hamam, F., Budge, S.M., 2010. Structured and specialty lipids in continuous packed column reactors:  
495 comparison of production using one and two enzyme beds. *Journal of the American Oil Chemists'  
496 Society* 87, 385-394.

497 Iyer, P.V., Ananthanarayan, L., 2008. Enzyme stability and stabilization—Aqueous and non-aqueous  
498 environment. *Process Biochem., Metabolic Engineering* 43, 1019–1032.  
499 <https://doi.org/10.1016/j.procbio.2008.06.004>



500 Jatoi, H.U.K., Goepel, M., Poppitz, D., Kohns, R., Enke, D., Hartmann, M., Gläser, R., 2021. Mass  
501 Transfer in Hierarchical Silica Monoliths Loaded With Pt in the Continuous-Flow Liquid-Phase  
502 Hydrogenation of p-Nitrophenol. *Front. Chem. Eng.* 3.

503 Ji, C., Hou, J., Wang, K., Zhang, Y., Chen, V., 2016. Biocatalytic degradation of carbamazepine with  
504 immobilized laccase-mediator membrane hybrid reactor. *J. Membr. Sci.* 502, 11–20.  
505 <https://doi.org/10.1016/j.memsci.2015.12.043>

506 Ji, C., Nguyen, L.N., Hou, J., Hai, F.I., Chen, V., 2017. Direct immobilization of laccase on titania  
507 nanoparticles from crude enzyme extracts of *P. ostreatus* culture for micro-pollutant degradation. *Sep.*  
508 *Purif. Technol.* 178, 215–223. <https://doi.org/10.1016/j.seppur.2017.01.043>

509 Jing, X., Zhang, X., Bao, J., 2009. Inhibition Performance of Lignocellulose Degradation Products on  
510 Industrial Cellulase Enzymes During Cellulose Hydrolysis. *Appl. Biochem. Biotechnol.* 159, 696.  
511 <https://doi.org/10.1007/s12010-009-8525-z>

512 Jungreuthmayer, C., Steppert, P., Sekot, G., Zankel, A., Reingruber, H., Zanghellini, J., Jungbauer, A.,  
513 2015. The 3D pore structure and fluid dynamics simulation of macroporous monoliths: High  
514 permeability due to alternating channel width. *J. Chromatogr. A* 1425, 141–149.  
515 <https://doi.org/10.1016/j.chroma.2015.11.026>

516 Kanakaraju, D., Glass, B.D., Oelgemöller, M., 2018. Advanced oxidation process-mediated removal of  
517 pharmaceuticals from water: A review. *J. Environ. Manage.* 219, 189–207.  
518 <https://doi.org/10.1016/j.jenvman.2018.04.103>

519 Kerrigan, J.F., Sandberg, K.D., Engstrom, D.R., LaPara, T.M., Arnold, W.A., 2018. Sedimentary record of  
520 antibiotic accumulation in Minnesota Lakes. *Sci. Total Environ.* 621, 970–979.  
521 <https://doi.org/10.1016/j.scitotenv.2017.10.130>

522 Kidak, R., Doğan, Ş., 2018. Medium-high frequency ultrasound and ozone based advanced oxidation  
523 for amoxicillin removal in water. *Ultrason. Sonochem.*, SI: ESS-15, 2016, Istanbul 40, 131–139.  
524 <https://doi.org/10.1016/j.ultsonch.2017.01.033>

525 Llorca, M., Rodríguez-Mozaz, S., Couillerot, O., Panigoni, K., de Gunzburg, J., Bayer, S., Czaja, R.,  
526 Barceló, D., 2015. Identification of new transformation products during enzymatic treatment of  
527 tetracycline and erythromycin antibiotics at laboratory scale by an on-line turbulent flow liquid-  
528 chromatography coupled to a high resolution mass spectrometer LTQ-Orbitrap. *Chemosphere* 119,  
529 90–98. <https://doi.org/10.1016/j.chemosphere.2014.05.072>

530 Lloret, L., Eibes, G., Feijoo, G., Moreira, M.T., Lema, J.M., 2012. Continuous operation of a fluidized bed  
531 reactor for the removal of estrogens by immobilized laccase on Eupergit supports. *J. Biotechnol.*,  
532 *Current research and future perspectives of Applied Biotechnology* 162, 404–406.  
533 <https://doi.org/10.1016/j.jbiotec.2012.04.007>

534 Meyers, J.J., Liapis, A.I., 1999. Network modeling of the convective flow and diffusion of molecules  
535 adsorbing in monoliths and in porous particles packed in a chromatographic column. *J. Chromatogr. A*  
536 852, 3–23. [https://doi.org/10.1016/s0021-9673\(99\)00443-4](https://doi.org/10.1016/s0021-9673(99)00443-4)

537 Nguyen, L.N., Hai, F.I., Dosseto, A., Richardson, C., Price, W.E., Nghiem, L.D., 2016. Continuous  
538 adsorption and biotransformation of micropollutants by granular activated carbon-bound laccase in a  
539 packed-bed enzyme reactor. *Bioresour. Technol.*, Special Issue on Challenges in Environmental Science  
540 and Engineering (CESE-2015) 210, 108–116. <https://doi.org/10.1016/j.biortech.2016.01.014>

541 Nyanhongo, G.S., Nugroho Prasetyo, E., Herrero Acero, E., Guebitz, G.M., 2012. Engineering Strategies  
542 for Successful Development of Functional Polymers Using Oxidative Enzymes. *Chemical Engineering &*  
543 *Technology* 35, 1359-1372.

544 Ortner, A., Huber, D., Haske-Cornelius, O., Weber, H.K., Hofer, K., Bauer, W., Nyanhongo, G.S., Guebitz,  
545 G.M., 2015. Laccase mediated oxidation of industrial lignins: Is oxygen limiting? *Process Biochemistry*  
546 50, 1277-1283.

547 Parra Guardado, A.L., Belleville, M.-P., Rostro Alanis, M. de J., Parra Saldivar, R., Sanchez-Marcano, J.,  
548 2019. Effect of redox mediators in pharmaceuticals degradation by laccase: A comparative study.  
549 *Process Biochem.* 78, 123–131. <https://doi.org/10.1016/j.procbio.2018.12.032>

550 Patel, S.K.S., Kalia, V.C., Choi, J.H., Haw, J.R., Kim, I.W., Lee, J.K., 2014. Immobilization of Laccase on  
551 SiO<sub>2</sub> Nanocarriers Omproves Its Stability and Reusability. *J. Microbiol. Biotechnol.* 24, 639–647.  
552 <https://doi.org/10.4014/jmb.1401.01025>

553 Piao, M., Zou, D., Ren, X., Gao, S., Qin, C., Piao, Y., 2019. High efficiency biotransformation of bisphenol  
554 A in a fluidized bed reactor using stabilized laccase in porous silica. *Enzyme Microb. Technol.* 126, 1–8.  
555 <https://doi.org/10.1016/j.enzmictec.2019.03.006>

556 Rajapaksha, A.U., Dilrukshi Premarathna, K.S., Gunarathne, V., Ahmed, A., Vithanage, M., 2019. 9 -  
557 Sorptive removal of pharmaceutical and personal care products from water and wastewater, in:  
558 Prasad, M.N.V., Vithanage, M., Kapley, A. (Eds.), *Pharmaceuticals and Personal Care Products: Waste*  
559 *Management and Treatment Technology*. Butterworth-Heinemann, pp. 213–238.  
560 <https://doi.org/10.1016/B978-0-12-816189-0.00009-3>

561 Rocha, L.S., Pereira, D., Sousa, É., Otero, M., Esteves, V.I., Calisto, V., 2020. Recent advances on the  
562 development and application of magnetic activated carbon and char for the removal of  
563 pharmaceutical compounds from waters: A review. *Sci. Total Environ.* 718, 137272.  
564 <https://doi.org/10.1016/j.scitotenv.2020.137272>

565 Sadeghzadeh, S., Ghobadi Nejad, Z., Ghasemi, S., Khafaji, M., Borghei, S.M., 2020. Removal of  
566 bisphenol A in aqueous solution using magnetic cross-linked laccase aggregates from *Trametes*  
567 *hirsuta*. *Bioresour. Technol.* 306, 123169. <https://doi.org/10.1016/j.biortech.2020.123169>

568 Sebai, W., Ahmad, S., Belleville, M.-P., Boccheciampe, A., Chaurand, P., Levard, C., Brun, N., Galarneau,  
569 A., Sanchez-Marcano, J., 2022. Biocatalytic Elimination of Pharmaceuticals Found in Water With  
570 Hierarchical Silica Monoliths in Continuous Flow. *Front. Chem. Eng.* 4.

571 Sheldon, R.A., 2007. Enzyme immobilization: The quest for optimum performance. *Adv. Synth. Catal.*  
572 349, 1289–1307. <https://doi.org/10.1002/adsc.200700082>

573 Singh Arora, D., Kumar Sharma, R., 2010. Ligninolytic Fungal Laccases and Their Biotechnological  
574 Applications. *Appl. Biochem. Biotechnol.* 160, 1760–1788. <https://doi.org/10.1007/s12010-009-8676-y>

575 Tallarek, U., Leinweber, F.C., Seidel-Morgenstern, A., 2002. Fluid Dynamics in Monolithic Adsorbents:  
576 Phenomenological Approach to Equivalent Particle Dimensions. *Chem. Eng. Technol.* 25, 1177–1181.  
577 [https://doi.org/10.1002/1521-4125\(20021210\)25:12<1177::AID-CEAT1177>3.0.CO;2-V](https://doi.org/10.1002/1521-4125(20021210)25:12<1177::AID-CEAT1177>3.0.CO;2-V)

578 Thiebault, T., Boussafir, M., Le Milbeau, C., 2017. Occurrence and removal efficiency of  
579 pharmaceuticals in an urban wastewater treatment plant: Mass balance, fate and consumption  
580 assessment. *J. Environ. Chem. Eng.* 5, 2894–2902. <https://doi.org/10.1016/j.jece.2017.05.039>

581 Verlicchi, P., Al Aukidy, M., Zambello, E., 2012. Occurrence of pharmaceutical compounds in urban  
582 wastewater: Removal, mass load and environmental risk after a secondary treatment—A review. *Sci.*  
583 *Total Environ.*, Special Section - Arsenic in Latin America, An Unrevealed Continent: Occurrence, Health  
584 Effects and Mitigation 429, 123–155. <https://doi.org/10.1016/j.scitotenv.2012.04.028>

585 Zdarta, J., Feliczak-Guzik, A., Siwińska-Ciesielczyk, K., Nowak, I., Jesionowski, T., 2020. Mesostructured  
586 cellular foam silica materials for laccase immobilization and tetracycline removal: A comprehensive  
587 study. *Microporous Mesoporous Mater.* 291, 109688.  
588 <https://doi.org/10.1016/j.micromeso.2019.109688>

589 Zdarta, J., Meyer, A.S., Jesionowski, T., Pinelo, M., 2018. Developments in support materials for  
590 immobilization of oxidoreductases: A comprehensive review. *Adv. Colloid Interface Sci.* 258, 1–20.  
591 <https://doi.org/10.1016/j.cis.2018.07.004>

592 Zhang, Y., Ge, J., Liu, Z., 2015. Enhanced Activity of Immobilized or Chemically Modified Enzymes. *ACS*  
593 *Catal.* 5, 4503–4513. <https://doi.org/10.1021/acscatal.5b00996>

594 Zheng, F., Cui, B.K., Wu, X.J., Meng, G., Liu, H.X., Si, J., 2016. Immobilization of laccase onto chitosan  
595 beads to enhance its capability to degrade synthetic dyes. *Int. Biodeterior. Biodegrad.* 110, 69–78.  
596 <https://doi.org/10.1016/j.ibiod.2016.03.004>

597

598

599